# Monte-Carlo simulation for range intensity profile of underwater range gated imaging

Zhang, Yue, Wang, Xinwei, Zhou, Yan

Yue Zhang, Xinwei Wang, Yan Zhou, "Monte-Carlo simulation for range intensity profile of underwater range gated imaging," Proc. SPIE 12169, Eighth Symposium on Novel Photoelectronic Detection Technology and Applications, 12169BA (27 March 2022); doi: 10.1117/12.2626771

SPIE.

Event: Eighth Symposium on Novel Photoelectronic Detection Technology and Applications, 2021, Kunming, China

# Monte-Carlo Simulation for Range Intensity Profile of Underwater Range Gated Imaging

Yue Zhang[a, b], Xinwei Wang[*a, b, c, d], and Yan Zhou[a, b, c]

[a]Optoelectronic System Laboratory, Institute of Semiconductors, CAS, Beijing 100083, China
[b]College of Materials Science and Opto-Electronics Technology, University of Chinese Academy of Sciences, Beijing 100049, China
[c]School of Electronic, Electrical and Communication Engineering, University of Chinese Academy of Sciences, Beijing 100049, China
[d]Southern Marine Science and Engineering Guangdong Laboratory (Zhuhai), Zhuhai 519000, China

## ABSTRACT

Underwater range gated imaging (RGI) technique has been widely studied since it can well suppress scattering noise from water. The range intensity profile (RIP) plays a vital role in the image quality and range accuracy of underwater 2D and 3D RGI. The existing theoretical analysis for underwater RIPs mainly considers the attenuation effect of water on light propagation. However, it does not take into account the water scattering effect, and thus cannot fully reveal the characteristics of RIPs in underwater RGI. This paper has proposed a RIP analysis method for underwater RGI based on Monte Carlo method. The simulation results show that the water scattering significantly affects the properties of RIP, making it broadening and smoothing. The proposed method and conclusion will contribute to the design of underwater RGI systems, as well as optimizing their operating parameters.

**Keywords:** underwater range gated imaging, range intensity profile, Monte Carlo simulation

## 1. INTRODUCTION

Underwater optical imaging has become a research hotspot in recent years since its high resolution, fast imaging speed and obvious image characteristics. However, due to the strong absorption and scattering effect of water, the working distance of underwater optical imaging is limited and the image quality suffers. The target optical signal is decayed by the absorption effect of water. The scattering effect of water changes the direction of signal light and generates backscattering noise. Thus, underwater optical images are usually blurred and noisy. Their signal-to-noise ratio (SNR) and contrast is low, which can hardly meet the application requirements. Therefore, it's important to overcome the absorption and scattering effects of water and improve the quality of underwater optical images.

Range gated imaging (RGI) is a technology widely used in underwater optical imaging, since it can effectively suppress the backscattered noise from water. The working distance of underwater RGI can reach up to $3 \sim 7$ attenuation lengths (ALs) in water, depending on different turbidity of water. In RGI, by appropriately choosing the pulse width of the pulsed light source, the width of the detector's gate and the gate opening time delay, only the light in the range of interest (ROI) surrounding the target will be received by the detector. Since the convolution effect of the light pulse and the detector gate, the intensity of light received by the detector differs at different ranges, forming the range intensity profile (RIP). The light received by the detector is composed of the reflected light of target and scattering noise in the ROI, both are modulated by the RIP. RIP is a function related to light pulse, detector gate, water quality, and target distance. The shape of RIP curve determines the imaging quality of RGI. Moreover, since the RIP curve associates range and image intensity together, it becomes possible to obtain distance information of target from range gated images. Many underwater range gated 3D

*Corresopnding author: wangxinwei@semi.ac.cn

Eighth Symposium on Novel Photoelectronic Detection Technology and Applications, edited by Junhong Su, Lianghui Chen, Junhao Chu, Shining Zhu, Qifeng Yu, Proc. of SPIE Vol. 12169, 12169BA
 · 0277-786X · doi: 10.1117/12.2626771

imaging technologies rely on RIP. The accuracy and precision of underwater RGI 3D imaging is greatly affected by RIP. Therefore, the RIP curve plays a key role in underwater range gated imaging.

Over the years, there are a lot of research based on RIP character of RGI. Busck *et al.*[1] present a new 3-D optical underwater imaging method via RIP weighted average of scanning range gated images. Tan *et al.*[2] studied reflected image temporal profile (RITP) of underwater RGI, which is an equivalence of RIP. From the RITP character they found tail RITP region shows more reduction in the unwanted backscatter effects than the target intensity. Laurenzis *et al.*[3] present a technique to achieve super-resolution three-dimensional range gated imaging by analyzing the trapezoidal RIP. Wang *et al.*[4] developed the underwater three-dimensional range gated laser imaging based on triangular RIP. Kabashnikov *et al.*[5] proposed a method for distance determination of underwater RGI by finding the maximum position of RIP curve. Wang *et al.*[6] proposed underwater 3D deblurring-gated range-intensity correlation imaging method based on light propagation property in water. Wang *et al.*[7] proposed range-intensity-profile prior dehazing method for improving the image quality of underwater RGI. Wang *et al.*[8] proposed deblurring method for underwater 2D and 3D range gated imaging based on RIP character.

However, since the RIP is affected by various factors related to the light source, transmission media, target character, and the detector, it is quite difficult to get the analytical solution, even though for a specific RGI system under certain condition. The RIP used in RGI analysis is usually from simplified model, where some factors are omitted. The lidar equation is widely used for RIP analysis of RGI.[9] The general lidar equation assumes that light travels in a straight line, and the light energy received by the detector is caused by backscattering and target reflection. However, the propagation of light in water undergoes multiple scattering, which deviates its propagation direction, delays its travelling time. The scattering effect affects RIP but is not counted in general lidar equation. To address this problem, Walker and McLean[10] proposed lidar equations for turbid media with pulse stretching, which takes the beam spreading of underwater light propagation into account. In this paper, the RIP character of RGI is analyzed by Monte Carlo simulation method. The basic principles of underwater RGI and a simplified theoretical model of RIP is introduced, the Monte Carlo simulation method for underwater RGI is elaborated, and then the characteristics of RIP for underwater RGI and its related factors is analysed via Monte Carlo method.

## 2. UNDERWATER RANGE GATED IMAGING

### 2.1 Underwater range gated imaging

In underwater active imaging process, light is emitted from the light source, absorbed and scattered by water or other particles, reaching the target and then reflected. The reflected light enters the optical system and is finally received by the detector. In underwater RGI system, shown in Fig. 1, the light source is usually a pulsed LED or laser while the detector has a gated module. The pulsed light source and gated detector are synchronized. Therefore, not all photons can enter the detector. The detector's gate remains closed until the first-emitted-photon is reflected by the target and reaches the detector. After that, the gate remains open, until the last-emitted-photon reflected by the target and reaches the detector. Then the gate is closed. Photons backscattered before reaching the target take less time and reach the detector before the gate is open. Photons forward scattered but hit the target take more time to reach the detector after the gate closed. Thus, they can hardly be received by the detector. However, a few scattered photons can still be received by the detector during the gate opening time, causing the blurring and noisy effect in underwater RGI images. The signal light and the scattering light are both modulated by RIP.

### 2.2 Range intensity profile

In underwater RGI process, assuming the light pulse is rectangular shape with the width of $t_L$, the first photon emits at time 0, and the detector gate is rectangular shape with gate time of $t_G$. The time delay of the gated detector is set according to the volume of interest (VOI). Assuming that the target is located $R_T$ away from the imaging system, the time delay $\tau = 2R_T/c_0$, where $c_0$ is the light speed in water. Not considering the absorption and scattering effect of water, the theoretical RIP is the convolution of the light pulse and the detector gate,

$$I(R) = \int_{-\infty}^{\infty} P\left(t - 2\frac{R}{c_0}\right) G(t-\tau)dt \tag{1}$$

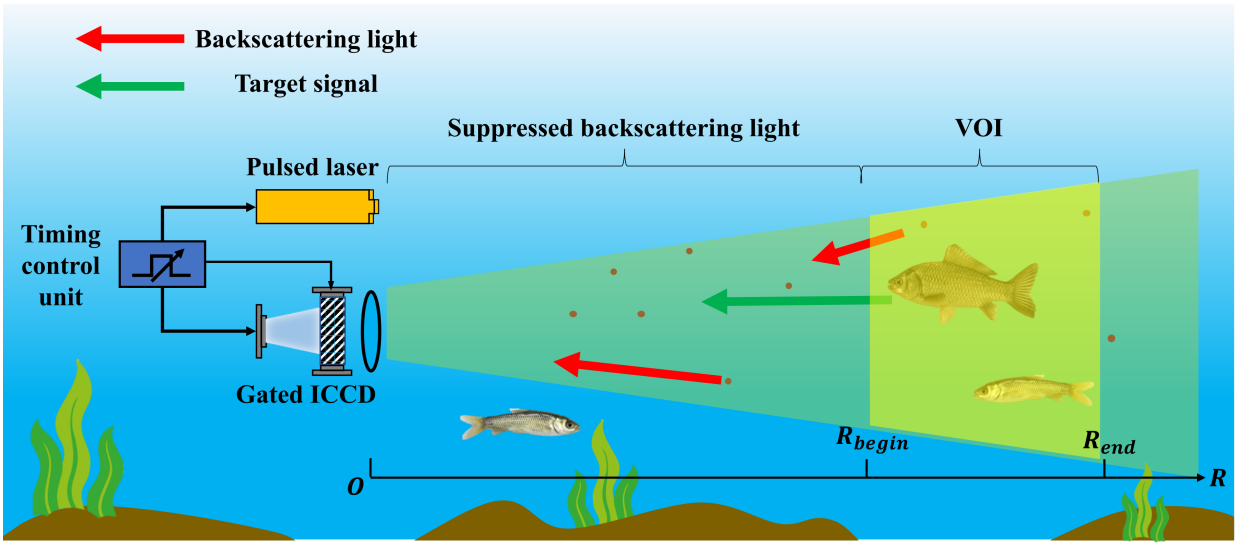


Figure 1. Underwater Range gated imaging system, comprising pulsed laser, gated ICCD, timing control unit, etc. By synchronizing the laser pulse, detector gate and gate delay, only the signal light from the target and backscattering light within volume of interest (VOI) can be record by ICCD. The backscattering light out of VOI is suppressed.

where $I(R)$ is intensity as a function of range, $P(t-2R/c_0)$ is the light pulse function, $G(t-\tau)$ is the detector's gate function. Usually, without loss of generality, $P(t)$ and $G(t)$ are chosen to be rectangular pulse function,

$$P(t) = \text{rect}\left(\frac{t-1/2t_L}{t_L}\right) = \begin{cases} 0, & otherwise \\ P_0, & 0 \le t < t_L \end{cases} \tag{2}$$

$$G(t) = \text{rect}\left(\frac{t-1/2t_G}{t_G}\right) = \begin{cases} 0, & otherwise \\ 1, & 0 \le t < t_G \end{cases} \tag{3}$$

where $P_0$ is the light power.

Shown in Fig. 2, with the different relationship between $t_L$ and $t_G$, the shape of RIP differs. When $t_L < t_G$, the shape of RIP is trapezoidal, and when $t_L = t_G$, the shape of RIP is triangular. Usually, it is not recommended to set $t_L > t_G$ since it is a waste of light energy. The theoretical RIP without underwater effect is widely used for underwater gated range-intensity-correlation imaging (GRICI). However, the absorption and scattering effect of water is not neglectable and thus RIP in underwater RGI is no longer perfect trapezoidal or triangular. Using the theoretical RIP without underwater effect, it is impossible to get the optimal time delay, VOI and other relevant parameters for underwater RGI system. Moreover, the range accuracy of underwater 3D gated imaging will also be affected.

To address the problem, RIP taking the underwater effect into account is proposed. According to Beer-Lambert law, the energy of light during underwater transmission decays exponentially with distance. The RIP of underwater RGI is suppressed by $\exp(-2cR)$. Considering that at different ranges, the illuminating spot just completely covers the target, that is, the light energy density received by the target is the same, the RIP function can be expressed as

$$I(R) = \exp\left(-2cR\right) \int_{-\infty}^{\infty} P\left(t - \frac{2R}{c_0}\right) \cdot G(t-\tau)dt \tag{4}$$

where $R$ is the range, $c$ is the attenuation coefficient of water. The factor 2 is because of the round-trip path of photon. Thus, the underwater RIP can be obtained. Fig. 3 shows the triangular RIP with water attenuation, where the light pulse is rectangular with width $t_L = 8.87$ns, the time delay $\tau = 35.5$ns, detector's gate time $t_G = t_L$. Figure 4 shows the trapezoidal RIP with water attenuation, where the light pulse is rectangular with width $t_L = 8.87$ns, the time delay $\tau = 31.0$ns, detector's gate time $t_G = 2t_L$. From Fig. 3 and Fig. 4, both

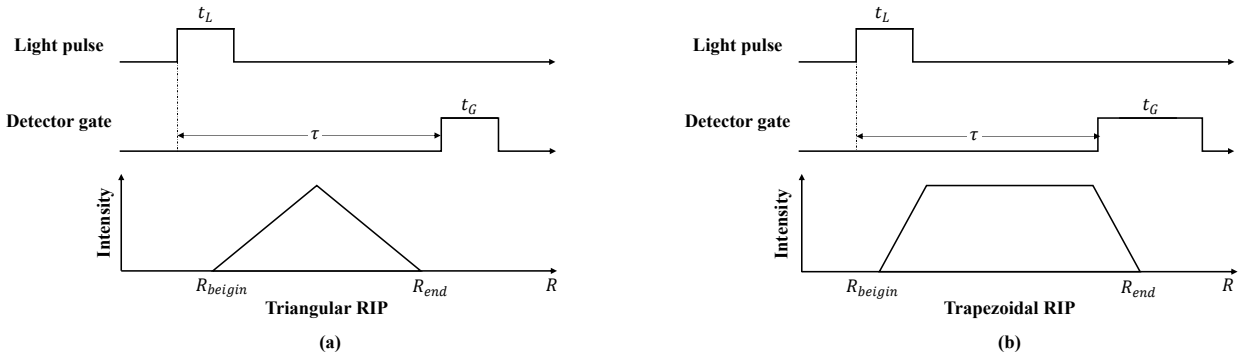


Figure 2. Theoretical RIP curve. (a) Triangular RIP when $t_L = t_G$. (b) Trapezoidal RIP when $t_L < t_G$.

the shape of triangular and trapezoidal RIPs is affected by water attenuation. The RIP curve is supressed due to the decay of light energy. For $t_G = t_L$, when the water attenuation coefficient $c$ is small ($< 0.5$), the maximum position of RIP curve remains unchanged. As the water attenuation coefficient $c$ increases ($> 0.5$), the maximum position of RIP curve moves left. This means the target distance $R_{max}$ that maximizes the light intensity received by the detector is no longer the position $R = 0.5\tau c$ calculated based on the time delay without water attenuation. The previous maximum position of RIP $R = 0.5\tau c$ now becomes a point of the curve where the RIP curve starts to drop rapidly as range increases. Similar character can be found for $t_G > t_L$, shown in Fig. 4.

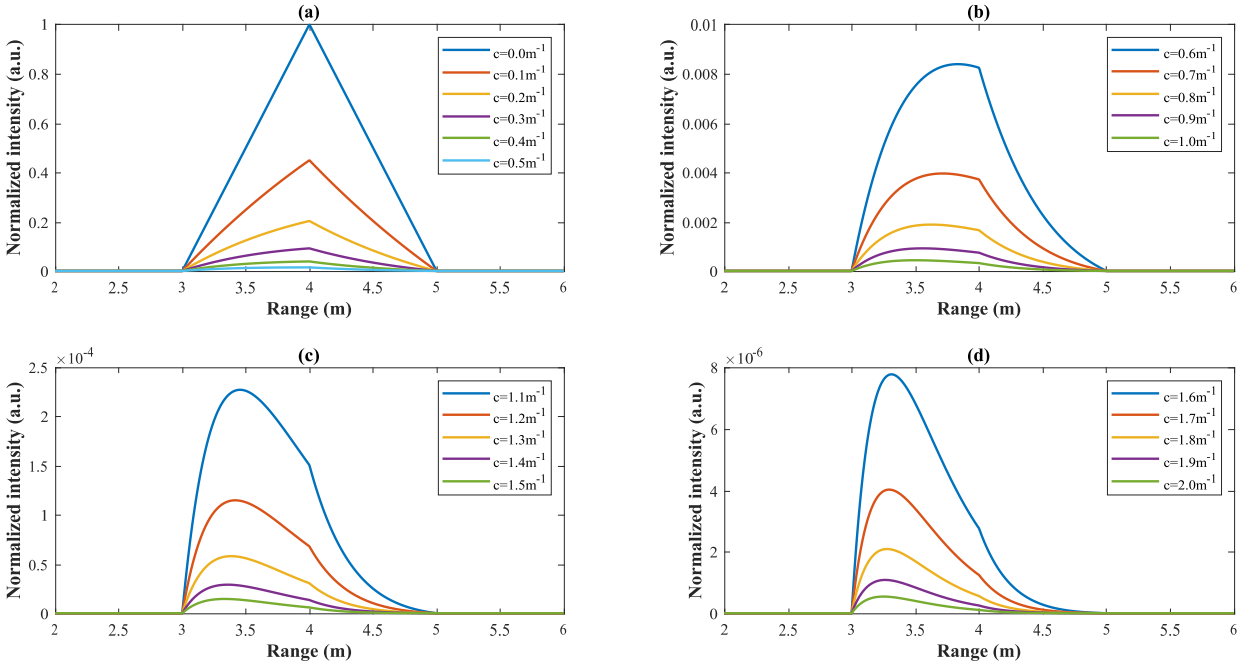


Figure 3. RIPs of underwater RGI, when $t_G = t_L$, with water attenuation. (a) RIPs at water attenuation coefficient $c = 0.0, 0.1, 0.2, 0.3, 0.4, 0.5\text{m}^{-1}$, (b) RIPs at water attenuation coefficient $c = 0.6, 0.7, 0.8, 0.9, 1.0\text{m}^{-1}$, (c) RIPs at water attenuation coefficient $c = 1.1, 1.2, 1.3, 1.4, 1.5\text{m}^{-1}$, (d) RIPs at water attenuation coefficient $c = 1.6, 1.7, 1.8, 1.9, 2.0\text{m}^{-1}$.

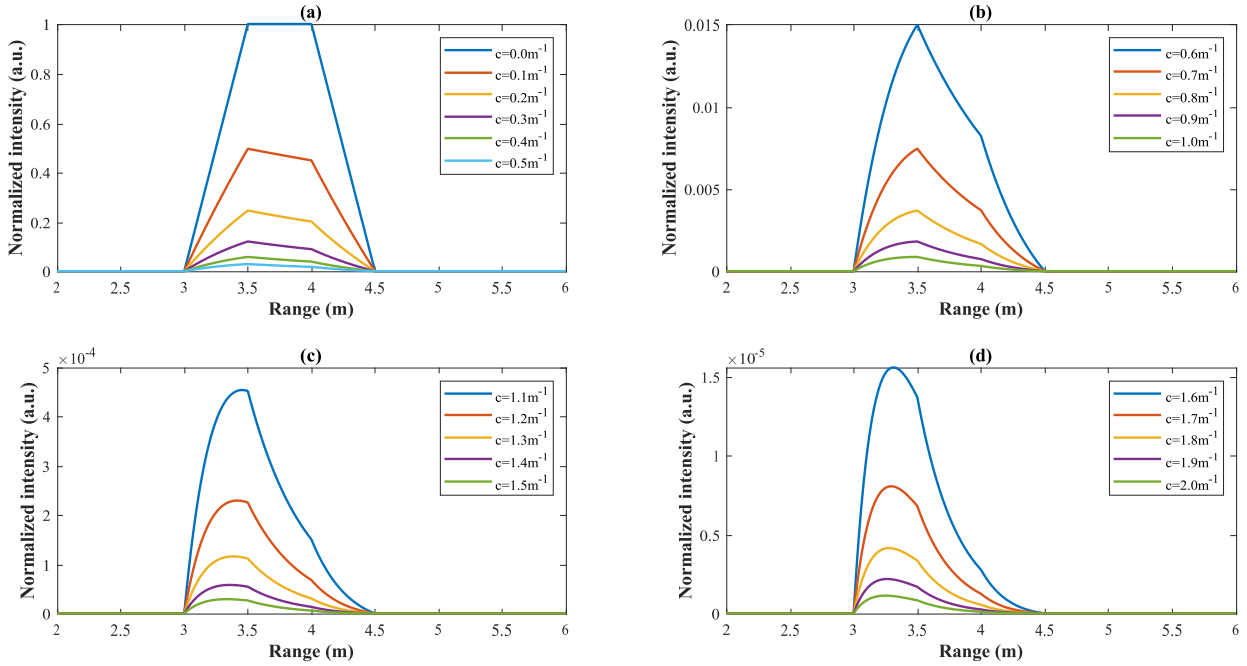


Figure 4. RIPs of underwater RGI, when $t_G = 2t_L$, with water attenuation. (a) RIPs at water attenuation coefficient $c = 0.0, 0.1, 0.2, 0.3, 0.4, 0.5\text{m}^{-1}$, (b) RIPs at water attenuation coefficient $c = 0.6, 0.7, 0.8, 0.9, 1.0\text{m}^{-1}$, (c) RIPs at water attenuation coefficient $c = 1.1, 1.2, 1.3, 1.4, 1.5\text{m}^{-1}$, (d) RIPs at water attenuation coefficient $c = 1.6, 1.7, 1.8, 1.9, 2.0\text{m}^{-1}$.

## 3. MONTE CARLO SIMULATION OF UNDERWATER RGI

### 3.1 Monte Carlo simulation of RGI process

Monte Carlo simulation is a physical-model-based method that can perform full-link simulation in the RGI process. As a random sampling method, Monte Carlo simulation treats each process in RGI as random sampling based on the approximation of the multiple scattering model. The simulation focuses on the light source, medium, target, and detector in RGI. Monte Carlo model believes that light is composed of individual virtual photons, and each photon travels independently. The algorithm workflow of Monte Carlo RGI simulation process is shown in Fig. 5.

For every photon, its initial position is sampled from the intensity distribution function of the light source. Here the uniform distribution is used as the density distribution function of the light source. Then calculate photon propagation step from the photon free path. The photon free path $l$ can be obtained by sampling the Beer-Lambert law through the inverse transform algorithm:

$$l = -\frac{\ln(r)}{c} \tag{5}$$

where $r$ is a uniform distributed random number, $c$ is the water attenuation coefficient. The energy of the photon will attenuate after a move. The energy attenuation of the photon is represented by the decay of the photon weight $W$. For each move, the photon weight W attenuates to be its $b/c$, where $c$ is the water attenuation coefficient and $b$ is the scattering coefficient. Photon may be scattered by the particles or inhomogeneous medium. The law of scattering is described by the scattering phase function, which shows the intensity distribution of scattered light at different angles, *i.e.*, the probability distribution of the photon being scattered to different angles. By sampling the scattering phase function, a single scattering process can be modeled. The commonly used scattering phase function is the Henyey-Greenstein phase function,[11] and the sampling result is:

$$\cos\theta = \frac{1}{2g}\left[1 + g^2 - \left(\frac{1-g^2}{1+g-2gr}\right)\right] \tag{6}$$

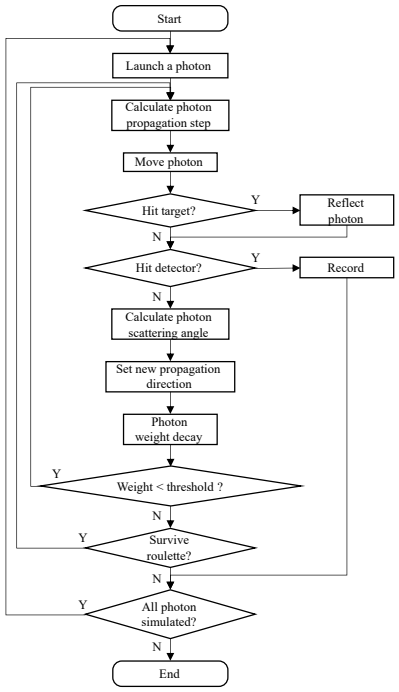


Figure 5. The algorithm workflow of Monte Carlo simulation for RGI.

where $\theta$ is the scattering angle, $r$ is another uniformly distributed random number, $g$ is the asymmetry factor. The azimuth $\varphi$ is uniformly distributed in $[0, 2\pi]$. After getting the scattering angle and the azimuth, the direction vector of the photon $(u_x, u_y, u_z)$ should be updated:

$$\begin{bmatrix} u_x \\ u_y \\ u_z \end{bmatrix} \leftarrow \begin{bmatrix} \frac{u_x u_z}{\sqrt{1-u_z^2}} & \frac{-u_y}{\sqrt{1-u_z^2}} & u_x \\ \frac{u_y u_z}{\sqrt{1-u_z^2}} & \frac{u_x}{\sqrt{1-u_z^2}} & u_y \\ -\sqrt{1-u_z^2} & 0 & u_z \end{bmatrix} \begin{bmatrix} \sin\theta\cos\varphi \\ \sin\theta\sin\varphi \\ \cos\theta \end{bmatrix}, u_z^2 < 1. \tag{7}$$

$$\begin{bmatrix} u_x \\ u_y \\ u_z \end{bmatrix} \leftarrow \begin{bmatrix} \sin\theta\cos\varphi \\ \sin\theta\sin\varphi \\ \frac{u_z}{|u_z|}\cos\theta \end{bmatrix}, u_z^2 \approx 1. \tag{8}$$

When propagating, the photon will undergo multiple moves, weight decay and scattering processes. If the photon hits the target, it will be reflected. The photon weight $W_{reflected}$ becomes:

$$W_{reflected} = W \cdot R(x, y) \tag{9}$$

where $R(x, y)$ is the reflective rate of the target at $(x, y)$. In our simulation, $R(x, y) = I_{gray}(x, y)$, which is the normalized grayscale target image at pixel position $(x, y)$. Photons reflected by the target or photons scattered by particles can reach the detector. The detector will record the position, travelling time and weight of the photon. Then a range-gated image $I_{rg}$ is generated:

$$I_{rg} = \mathrm{pdf}(x, y, W) \tag{10}$$

where $\mathrm{pdf}(x, y, W)$ is the density function of the detector collected photons in the pixel bin $(x \sim x + \Delta x, y \sim y + \Delta y)$, weighted by the photon weights $W$.

### 3.2 Simulation RIPs for underwater RGI

To investigate the RIP character of underwater RGI, we performed Monte Carlo simulations which take into account the water attenuation, the multiple scattering effect, etc. The parameters used in the simulations is shown in Tab. 1. These predefined parameters remain unchanged in all the simulations in this section. The normalized intensity is the average mean of the detector image $I_{rg}$.

Table 1. Predefined parameters of Monte Carlo simulation of RIP curve for underwater RGI.

| Name | Value |
|---|---|
| Light spot radius | 2.148 m |
| Target size | 3.336×2.706 $m^2$ |
| Asymmetry factor $g$ | 0.8 |
| Refractive index $n$ | 1.33 |
| Number of photons | 48,000,000 |

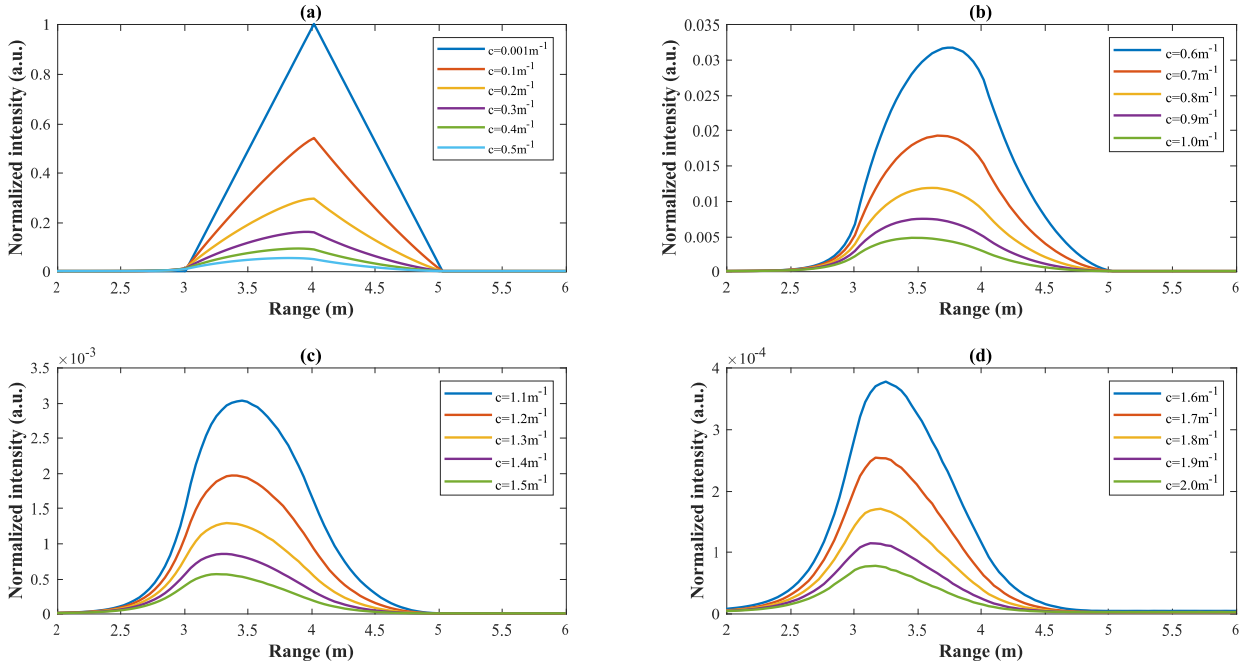


Figure 6. Simulated RIPs of underwater RGI, when $t_G = t_L$. (a) RIPs at water attenuation coefficient $c = 0.0, 0.1, 0.2, 0.3, 0.4, 0.5\text{m}^{-1}$, (b) RIPs at water attenuation coefficient $c = 0.6, 0.7, 0.8, 0.9, 1.0\text{m}^{-1}$, (c) RIPs at water attenuation coefficient $c = 1.1, 1.2, 1.3, 1.4, 1.5\text{m}^{-1}$, (d) RIPs at water attenuation coefficient $c = 1.6, 1.7, 1.8, 1.9, 2.0\text{m}^{-1}$.

We performed simulations of RIPs for underwater RGI when $t_G = t_L$ and $t_G = 2t_L$, the albedo $b/c$ is set to be 0.5. Fig. 6 shows the RIP curves when $t_G = t_L = 8.87$ns, the time delay $\tau = 35.5$ns at different water attenuation coefficients. Fig. 7 shows the RIP curves when $t_G = 2t_L = 8.87$ns, the time delay $\tau = 31.0$ns at different water attenuation coefficients.

The simulation results show some differences from the theoretical ones in Fig. 3 and Fig. 4. The RIPs calculated by Monte Carlo simulations present broadening effect. The theoretical RIPs show that only in the range of $0.5c \cdot [\tau, \tau + t_L + t_G]$ can the light be recorded by the detector. However, the simulated RIPs show that the light can be recorded by the detector in a larger range. Shown in Fig. 8(a), both the theoretical and simulated results show that 50%-peak-width of RIP decrease as attenuation coefficient increases. However, the

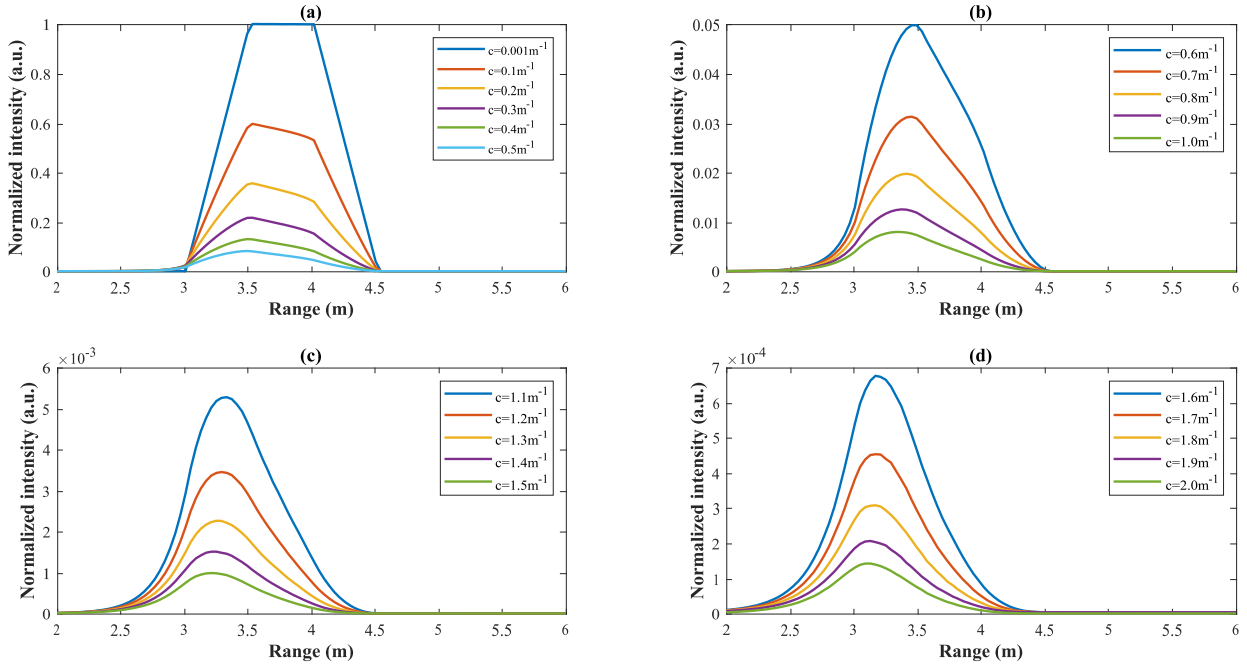


Figure 7. Simulated RIPs of underwater RGI, when $t_G = 2t_L$. (a) RIPs at water attenuation coefficient $c = 0.0, 0.1, 0.2, 0.3, 0.4, 0.5\text{m}^{-1}$, (b) RIPs at water attenuation coefficient $c = 0.6, 0.7, 0.8, 0.9, 1.0\text{m}^{-1}$, (c) RIPs at water attenuation coefficient $c = 1.1, 1.2, 1.3, 1.4, 1.5\text{m}^{-1}$, (d) RIPs at water attenuation coefficient $c = 1.6, 1.7, 1.8, 1.9, 2.0\text{m}^{-1}$.

simulated 5%-peak-width of RIP increases as attenuation coefficient increases. The increased range is owing to the scattering effect, containing both forward and backward scattering. The broadening effect means more scattering noise is introduced to the underwater RGI system when the water quality is poor. To suppress the noise, the underwater RGI system should be designed to have a smaller pulse width and gate time, when operating in the turbid water. Fig. 8(b) shows the simulated relationship between RGI image contrast and pulse width, under the attenuation coefficient of $c = 1\text{m}^{-1}$, when $t_G = t_L$. The relationship shows the image contrast decreases exponentially as pulse width increases, confirming the conclusion drawn by RIP analysis. The simulated RIPs are smoother, compared to the theoretical ones. There is no mutation point in the simulated RIPs. The smoothing effect is also caused by scattering. Therefore, it is no longer valid to get the target distance via analyzing the derivative of RIP curve.

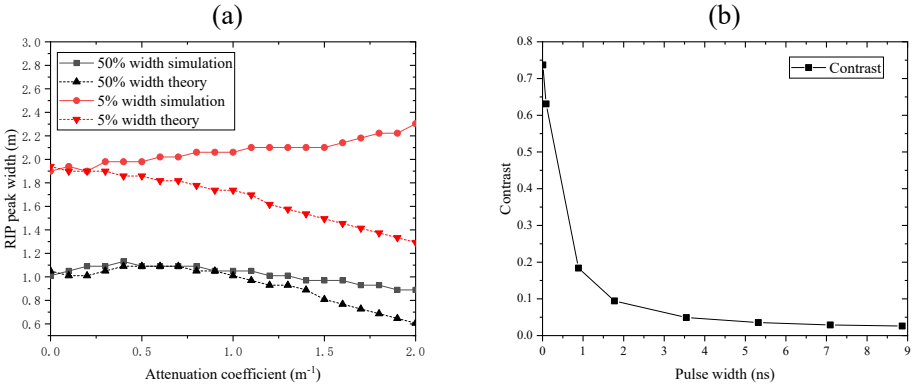


Figure 8. (a) The theoretical and simulated 50%-peak-width and 5%-peak-width of RIPs under different attenuation coefficient. (b) The image contrast of underwater RGI, under different pulse width. The attenuation coefficient $c = 1\text{m}^{-1}$, $t_G = t_L$.

## 4. CONCLUSION AND DISCUSSION

In this paper, a Monte-Carlo-simulation-based RIP characteristics of underwater RGI analysis has been presented. The simulation results show that water scattering significantly affects the characteristics of RIP, making the RIP broadening and smoothing. The simulation RIPs are more in line with the performance of the actual systems than the theoretical ones. The simulation results provide a theoretical basis for optimizing the parameters of underwater RGI systems. There are still many factors related to underwater RGI that have not been considered, such as albedo, asymmetry factor, field of view, etc. Related experiments need to be performed to verify the validity of the simulation results. This work will be carried out in our future research.

## ACKNOWLEDGMENTS

The authors acknowledge the financial fundings of this work, including National Natural Science Foundation of China (NSFC) (61875189, 62005264), Strategic Priority Program of the Chinese Academy of Sciences (XDC03060103, XDA22030205).

## REFERENCES

[1] Busck, J., "Underwater 3-D optical imaging with a gated viewing laser radar," *Optical Engineering* **44**(11), 116001 (2005).

[2] Tan, C., Seet, G., Sluzek, A., and He, D., "A novel application of range-gated underwater laser imaging system (ULIS) in near-target turbid medium," *Optics and Lasers in Engineering* **43**(9), 995–1009 (2005).

[3] Laurenzis, M., Christnacher, F., and Monnin, D., "Long-range three-dimensional active imaging with superresolution depth mapping," *Optics Letters* **32**(21), 3146 (2007).

[4] Wang, X., Liu, X., Ren, P., Sun, L., Fan, S., Lei, P., and Zhou, Y., "Underwater three-dimensional range-gated laser imaging based on triangular-range-intensity profile spatial-correlation method," in [*SPIE/COS Photonics Asia*], Dai, Q. and Shimura, T., eds., 1002006 (2016).

[5] Kabashnikov, V. and Kuntsevich, B., "Distance determination based on the delay time-intensity profile analysis in range-gated imaging," *Applied Optics* **56**(30), 8378 (2017).

[6] Wang, M., Wang, X., Sun, L., Yang, Y., and Zhou, Y., "Underwater 3D deblurring-gated range-intensity correlation imaging," *Optics Letters* **45**(6), 1455 (2020).

[7] Wang, M., Wang, X., Zhang, Y., Sun, L., Lei, P., Yang, Y., Chen, J., He, J., and Zhou, Y., "Range-intensity-profile prior dehazing method for underwater range-gated imaging," *Optics Express* **29**(5), 7630 (2021).

[8] Xinwei, W., Liang, S., Minmin, W., Yuqing, Y., and Yan, Z., "Deblurring methods for underwater 2D and 3D range-gated imaging," *Infrared and Laser Engineering* **49**(2), 0203002–0203002 (2020).

[9] Youwei, H., Fengmei, C., Weiqi, J., and Su, Q., "Underwater pulsed laser range-gated imaging model and its effect on image degradation and restoration," *Optical Engineering* **53**(6), 061608 (2013).

[10] Walker, R. E. and McLean, J. W., "Lidar equations for turbid media with pulse stretching," *Applied Optics* **38**(12), 2384 (1999).

[11] Toublanc, D., "Henyey–Greenstein and Mie phase functions in Monte Carlo radiative transfer computations," *Applied Optics* **35**(18), 3270 (1996).